Engineering Geology 31 (1991) 249–276
Elsevier Science Publishers B.V., Amsterdam

Geophysical, geotechnical and hydrological investigations of a small landslide in the French Alps

J.P.T. Caris and Th.W.J. Van Asch

Department of Physical Geography, University of Utrecht, P.O. Box 80115, 3508 TC Utrecht, Netherlands

(Received December 18, 1990; revised version accepted June 25, 1991)

ABSTRACT

Caris, J.P.T. and Van Asch, Th.W.J., 1991. Geophysical, geotechnical and hydrological investigations of a small landslide in the French Alps. Eng. Geol., 31: 249–276.

Geophysical, geotechnical and hydrological surveys were conducted in the French Alps on a small landslide in black marl material to assess the stability. The geophysical survey, consisting of electromagnetic, geo-electric and refraction seismic measurements, was carried out to examine depth to the basal slip surface and relative differences in water content.

The data on the basal slip surface, together with geotechnical parameters (cohesion and angle of internal friction), were used to make a stability analysis. This analysis revealed that a groundwater level of 4 m below the ground surface is the critical threshold for reactivating the landslide.

The hydrological investigation, which entailed measurements of saturated permeability and pressure heads, indicated that instability depended on long-term wet conditions with little evapotranspiration.

INTRODUCTION

In many areas mass movements cause damage to roads, buildings, etc., and threaten human safety. Detailed hazard mapping gives a first necessary overview of sites prone to mass movement and can indicate possible major factors influencing the stability of slopes such as, for example, lithology, slope and hydrological conditions. However, more detailed information is needed to assess the stability of a specific site.

Geophysical methods may be a helpful tool in obtaining part of this detailed information because the application of these methods provides a means of rapid investigation of the number of relevant slope layers, as well as of the water content and thickness of individual layers. A detailed stability analysis may be made after these data have been supplemented by the necessary geotechnical (cohesion and angle of internal friction) and morphological (slip surfaces) parameters. Stability analysis yields groundwater levels that may cause initial failure and resliding. The outcome of the stability analysis may be combined with the results of a detailed

0013–7952/91/$03.50

hydrological investigation in order to evaluate the hydrological processes and the meteorological conditions influencing the stability of the slopes. In this paper the methods and results of such an approach for a small landslide in the French Alps are described.

THE STUDY AREA

The slope studied lies in the Riou-Bourdoux Valley, a tributary of the Ubaye river, situated about 4 km northwest of Barcelonnette (Fig.1). The Riou–Bourdoux Valley is notorious for the great mass movement activity which has taken place in the last few centuries (Anon., 1966). Bedrock in this area consists of highly erodable, Jurassic, clayey black marls, (Terres Noires) on the lower part of the slopes and chalky Flysch (Eocene nappe with dark marls at its base) on the higher parts. During Weichselian glaciation parts of the Terres Noires and Flysch were covered with morainic material (Salomé and Beukenkamp, 1988).

Stream correction works were carried out from the end of the last century until 1977 in order to stabilize the river profile of the Riou–Bourdoux. These consisted of drainage works, reforestation of the largest parts of the area and the placing of numerous small dams in the catchment area and larger ones in the channel. The numerous recent landslides prove that these measures have not been completely successful.

The climate is sub-mediterranean. Mean (1956–1980) precipitation and potential evapotranspiration figures for Barcelonnette are given in Fig.2. Since only mean monthly temperatures are available for calculating potential evapotranspiration these data only serve as a rough estimate (see Thornthwaite and Mather, 1957).

A map of the slide investigated, in which measuring sites and profiles, as well as morphological data, are depicted, is shown in Fig.3. Auger drillings and soil pits have revealed that the displaced landslide mass consists of a mixture of Terres Noires marls which are weathered to varying degrees. The textural composition of the material is given in Table I. Illite is the most abundant clay mineral, while traces of kaolinite and chlorite are present.

The slope examined has been reforested with pine trees. In contrast to the trees

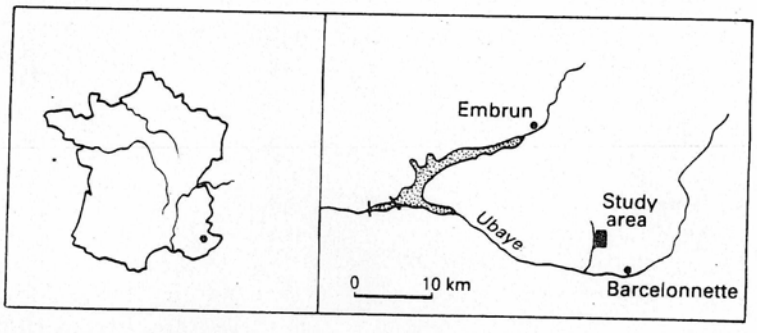

Fig.1. Location of the study area.

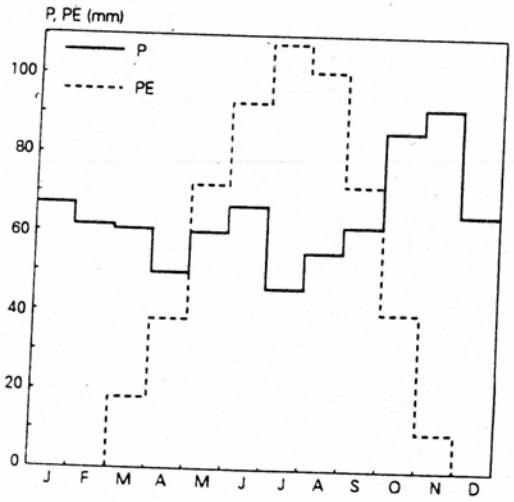

Fig.2. Mean monthly precipitation (P) and potential evapotranspiration (PE) for the Barcelonnette station. The means are calculated with data from 1956 to 1980. Potential evapotranspiration is calculated from mean monthly temperatures using Thornthwaite and Mather's (1957) method.

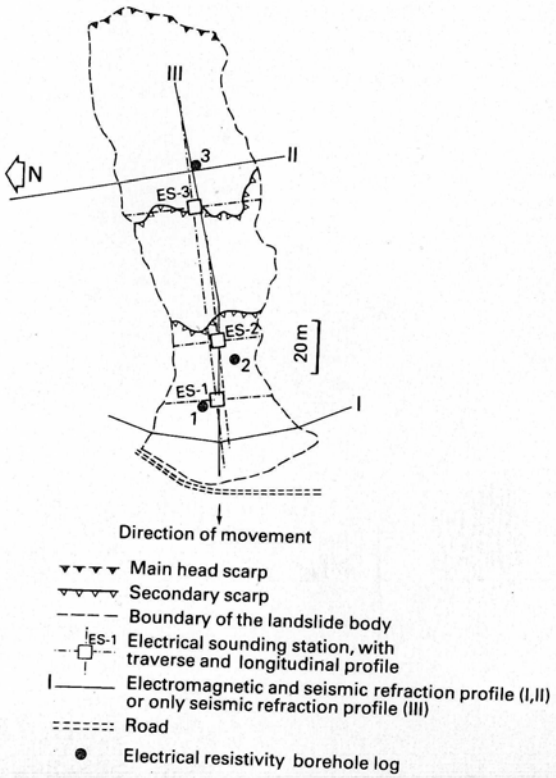

Fig.3. Map of the slide investigated showing scarps, measuring sites and profiles.

TABLE I

Mean values and standard deviation of some geotechnical properties of the Terres Noires colluvial material

Soil texture	
clay	35±5%
silt	55±5%
sand	2±1%
Plasticity index	10%±5
Dry bulk density	16.1±4.1 kNm^{-3}
Wet bulk density	19.4±4.0 kNm^{-3}
phi peak	27.4°±1.2°
Cohesion peak	14.1±4.2 kPa
phi residual	23.9°±2.8°
Cohesion residual	0
Compaction coefficient, C_c	0.234±0.020 (−)
Overconsolidation ratio, OCR	13.2±7.1 (−)

on the stable part of the slope, most trees on the landslide body are slanted and many have fallen down. The landslide has been stationary since 1980.

GEOPHYSICAL INVESTIGATION

Landslides often have the tendency to exhibit a considerable spatial variation in both depth to slip surface and in the nature of the slip debris. In addition, the situation is often complicated by the presence of complex, frequently perched, water tables. The reliability of the results of the geophysical investigation can be improved by using several methods at the same location and by calibration of the geophysical methods against borehole data (see Bogoslovsky and Ogilvy, 1977; Hutchinson, 1982). The electrical resistivity and refraction seismic measurements at the site described above were carried out in June, 1988, and April–May, 1989.

Resistivity measurements

Resistivity measurements may provide useful information because, depending on the ground and groundwater conditions, the electrical resistivity of a landslide mass may be higher or lower than that of the adjacent or underlying in situ strata. Significant resistivity differences within the landslide body may also be revealed.

"Shallow" resistivity soundings

A low-powered, direct current geo-electric apparatus was used to carry out shallow Schlumberger soundings to compare resistivities on the stable and unstable parts of the slope. Soundings were made with a maximum AB/2 of 15 m, both on the slide and on the stable slope to make this comparison. The results of six soundings (depicted in Fig.4) show that much higher resistivities are found on the stable part of the slope, reflecting the drier conditions. Furthermore, the resistivities indicate that, on the stable slope, relatively moist upper soil is separated from relatively moist

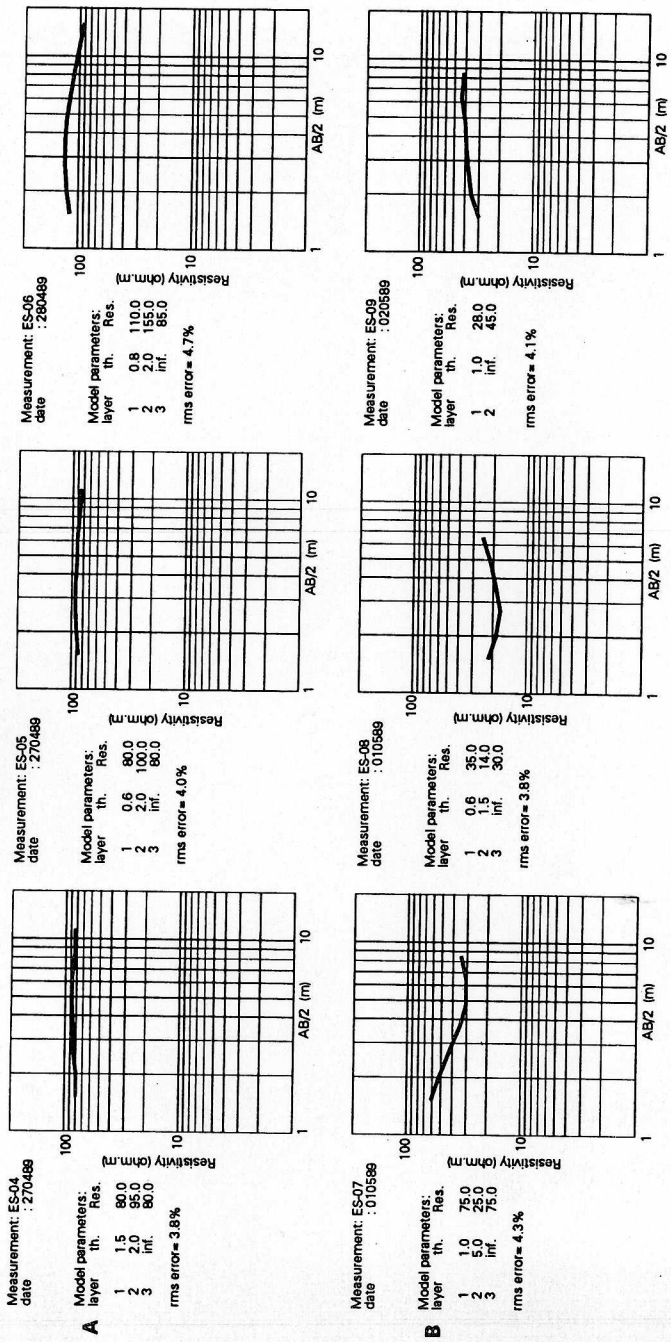

Fig.4. "Shallow" vertical electrical sounding curves measured with the Schlumberger array. A. curves measured at stable parts of the slope. B. curves measured at the landslide mass.

subsoil by a drier intermediate layer (higher resistivity), whereas more varied conditions appear in the slide.

Lateral resistivity changes

The Schlumberger soundings indicate a change of resistivity with depth at the measuring point. To explore the advantages of more detailed information about lateral resistivity changes, two profiles were measured across the landslide body with an EM34-3 electromagnetic instrument (Fig.3). Measurements were made every 2.5 m. Since the surface was irregular, the horizontal dipole mode (plane of the coils vertical) was used because in this mode the measurements are relatively insensitive to coil misorientation (McNeil, 1980). Coil spacings of 10, 20 and 40 m are possible. Since a coil spacing of 10 m (approximate exploration depth = 7.5 m) yields the highest resolution for detecting lateral changes in resistivity only these results will be discussed (Fig.5).

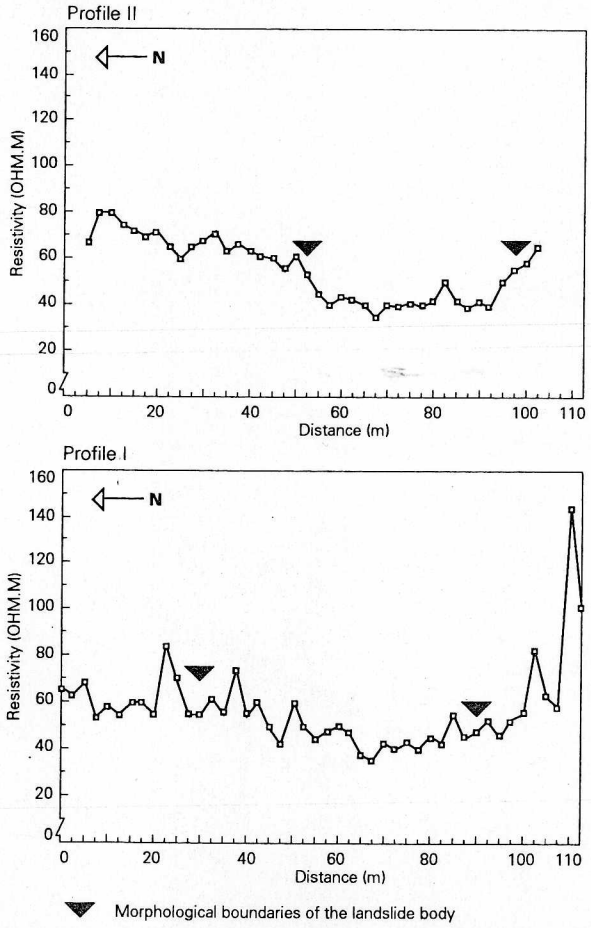

Fig.5. EM34 survey lines over the landslide body and adjacent stable parts of the slope. The measurements have been made in the horizontal dipole mode. Coil spacing is 10 m.

In profile II the boundary between the slide and the stable slope found by electromagnetic surveying coincides approximately with the morphological boundaries of the landslide body. This can probably be explained by a higher water content over the entire width of the landslide body.

Across the foot of the landslide (profile I) the results were different. Firstly, compared to profile II, there appears to be more short-distance variation in resistivity at both the stable and unstable parts of the slope. Secondly, the boundary between stable and unstable parts of the slope that may be drawn on the basis of the resistivities shown does not match the morphological boundaries of the landslide body. No explanation has been found for this anomaly. The lateral resistivity differences within the landslide body are interesting. The southern part exhibits much lower resistivities than the northern part. The differences in resistivity may be caused by:

(1) differences in lithology;
(2) differences in depth to bed rock;
(3) differences in water content within the landslide body.

However, since no significant changes in lithology have been observed in soil pits and boreholes, (1) does not apply. If case (2) applies, greater depths to bed rock should be found in the southern part of the landslide than in the northern part. The refraction seismic data (see below) indicate a lesser depth to bed rock in the southern part. Consequently, (2) does not apply. The observed differences in resistivity can, therefore, only be explained by moister conditions in the southern part of the landslide body; with drier conditions occurring in the northern part and the stable slope parts. This implies that the southern part of the foot of the landslide is possibly more prone to renewed movements than the northern part.

Resistivity borehole loggings

The above-mentioned geo-electric apparatus with electrical wires with open ends taped on to a PVC tube, was used to carry out electrical resistivity loggings in three percussion drilled, water-filled boreholes in the landslide mass. The principle of resistivity borehole logging is shown in Fig.6. The location of the boreholes is shown in Fig.3,and the results in Fig.7.

In the bore samples, reworked material could be distinguished from the weak schistose in-situ Terres Noires since the former lacks a laminated structure. In borehole 1, no in-situ Terres Noires were observed. In borehole 2 the bedrock was found at a depth of 8 m. In borehole 3 the situation is more complex, since material exhibiting a laminated structure was found from a depth of 4 m onwards. However, after examining the resistivity measurements and the seismic data (see below), it appears that only from a depth of approximately 7 m onwards, do in-situ Terres Noires occur. Therefore, the material from 4 to 7 m is thought to be a displaced chunk of weathered Terres Noires.

The resistivity logs show the following:

(1) An upper layer with a depth varying between 1 and 1.75 m, and a rapidly decreasing resistivity. Soil pits have revealed that visible shrinkage cracks partially filled with water extend down to a depth of approximately 1.5 m. The fact that the

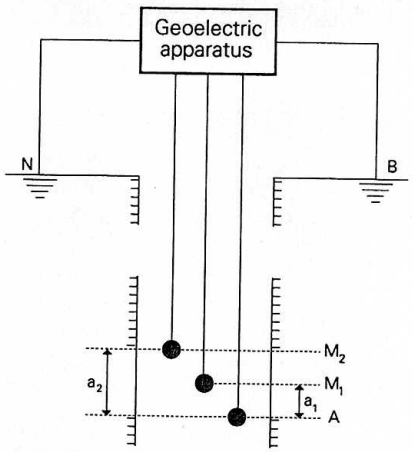

Fig.6. Principle of resistivity borehole logging. A and B = current electrodes; N, M_1 and M_2 = potential electrodes; a_1 = short normal, a_2 = long normal. Note: the short-normal will usually be influenced more by the borehole than the long-normal. Therefore, the long-normal will usually give a better measurement of the layer resistivity. The short-normal generally yields more accurate layer boundaries because of its higher resolution. In this case, the small differences in the results for short- and long-normal indicate that the long-normal measured the layer resistivity.

cracks become narrower and water-filled with increasing depth explains the observed rapid resistivity decrease in this upper layer.

(2) Resistivity logs 2 and 3 indicate that moisture accumulation takes place close to the bed rock and that the resistivity of the in-situ Terres Noires rises gradually. In accordance with the assumed extension of the borehole loggings (Fig.7), a resistivity of 75–80 Ohm·m for the first 2 m of the in-situ Terres Noires will be used in our resistivity models (see below).

"Deep" resistivity soundings

A more powerful geo-electric apparatus was used to determine the depth to bed rock underneath the slided mass. The Schlumberger array was used at three sites on the landslide body. At each site two soundings were made. One across the landslide body (maximum AB/2 = 25 m) and one along the axis of the landslide, that is, approximately along its direction of flow (maximum AB/2 = 40 m) (see Fig.3). Care was taken that the current electrodes were not placed outside the landslide body. Two soundings were taken at the same site but in perpendicular directions to examine whether the curves are typical of a given site. A lack of similarity in the results of these two soundings may indicate that these are influenced by lateral variation of the depth to the base of the landslide.

The resistivity loggings indicate a gradual rise in the resistivity of the in-situ Terres Noires. A resistivity of 75–80 Ohm·m was given to the first 2 m of the in-situ Terres Noires marls, as mentioned above. The deeper bedrock was assumed to have a resistivity of 150 Ohm·m. The results, as depicted in Fig.8, show that resistivity varies largely in the uppermost layer, which has desiccation cracks; whereas the results in both directions are sufficiently consistent for the deeper soil. This shows that the

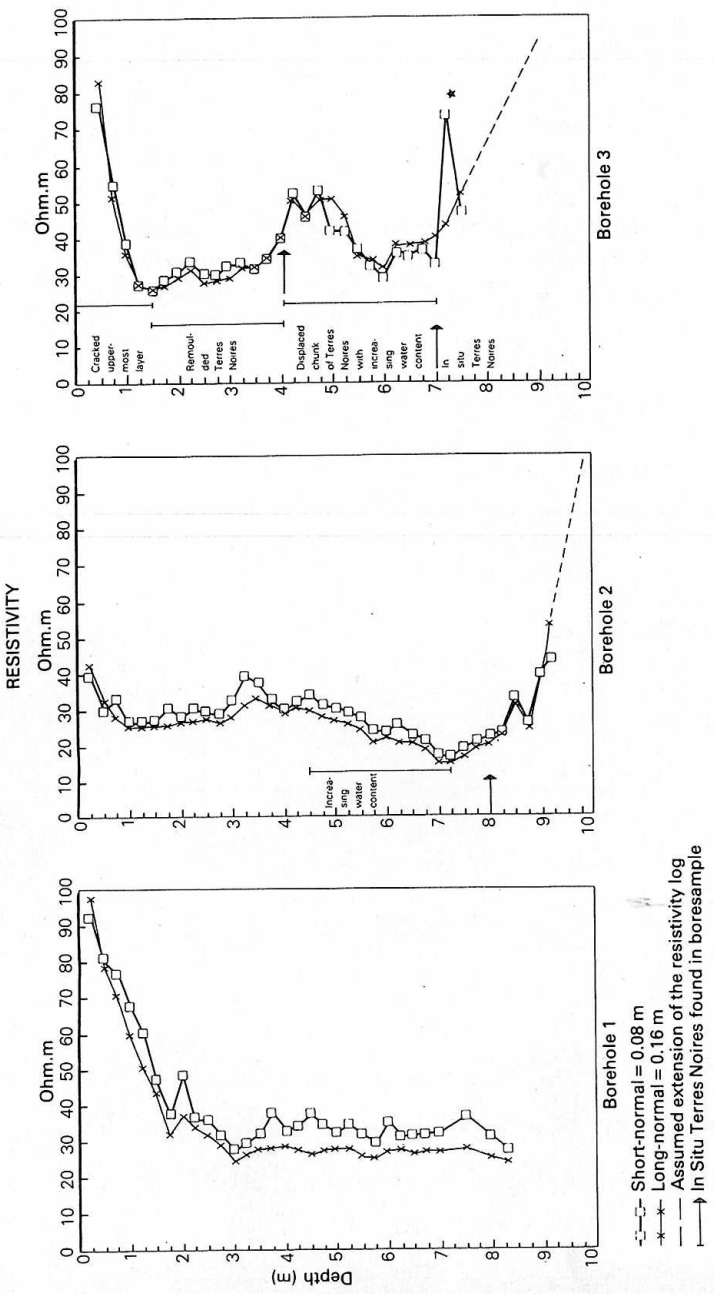

Fig.7. Measured soil resistivity–depth profiles in the landslide mass. Borehole $\Phi = 0.04$ m. * = probably a faulty measurement.

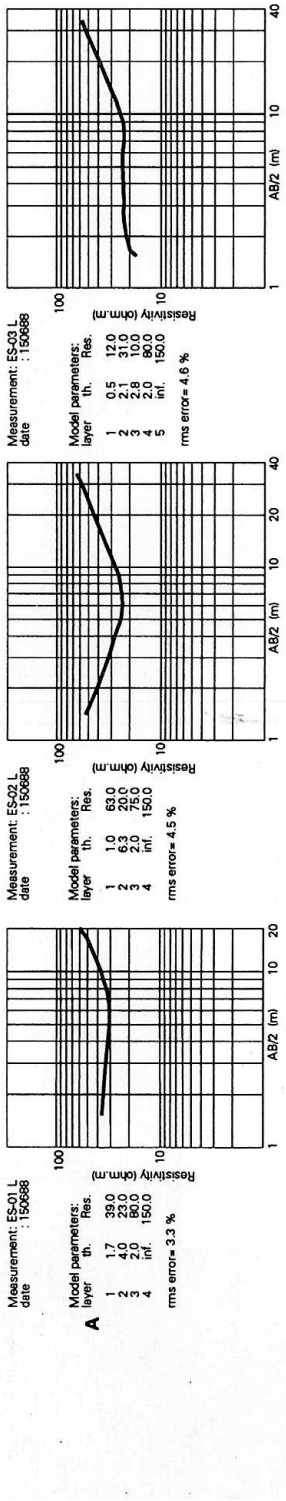

Fig. 8. "Deep" vertical electrical sounding curves measured with the Schlumberger array at the landslide site. A. Along the axis of the landslide. B. Across the landslide body. *ES*-01, *ES*-02 and *ES*- 03 = measuring stations.

results of the soundings are reliable. The soundings indicate that depth to bed rock varies approximately between 5.5 and 7.5 m.

Seismic refraction measurements

Seismic refraction is the most widely used of geophysical methods in landslide investigation. It utilises the tendency of a slipped mass to exhibit seismic velocities which are appreciably lower than those in the underlying in situ strata. The base of the landslide can be more-or-less clearly defined, depending on the degree of seismic contrast between these materials. However, this method is ineffective in cases where a thick layer of material of high seismic velocity (e.g., an intact rock slide mass or lava flow) overlies weaker material of low seismic velocity (e.g., weathered rock or alluvium). The presence of the latter is masked by the strong arrivals from its hard "roof" (Hutchinson, 1982).

A 12-channel seismograph was used for the measurements. To produce a seismic signal a sledge hammer was struck onto a steel plate placed on the surface. Three profiles were surveyed, forward and reverse: two traverse profiles coinciding with the electromagnetic profiles (Fig.3) and one longitudinal profile along the axis of the slide. Although the noise level was rather high (due to trees moving in the wind) the quality of the data was sufficient.

The seismic data were elaborated with the plus-minus method introduced by Hagedoorn (1959). A graphical method described by Helbig (1987) was used to work out the plus-minus method. Since this graphical method has not been described in international literature, the field arrangement, algorithm and field data are given in the Appendix. The results, shown in Fig.9, indicate that the base of the landslide varies in depth between approximately 4 and 9 m. The data also indicate that the depth to bed rock is greater on the unstable part of the slope than on the stable part.

Furthermore, a seismic velocity of 340 m/s found in the first layer implies that the major part of the landslide body is not saturated with water, since saturated sediment has a seismic velocity of around 1700 m/s. The term "major part of the landslide body" is used because hidden layers could still be present. Hidden layers are saturated layers, only a few meters thickness, from which the critical refraction event is overlooked due to the inaccuracy of the data.

Review of the results from the geophysical surveys

The results from resistivity and seismic refraction surveys and borings, indicate comparable depths to bed rock. The electrical resistivities and seismic velocities of the bed rock and the rock in the landslide body are given in Table II.

The geophysical investigations indicate that depth to the impervious Terres Noires varies between 4 and 9 m. Furthermore the data show that:

(1) there is a relatively moist layer close to bed rock;

(2) the landslide body mainly consists of unsaturated material;

(3) moisture is probably unevenly distributed over the foot of the landslide body.

The different surveys indicate comparable depths to bed rock and therefore the

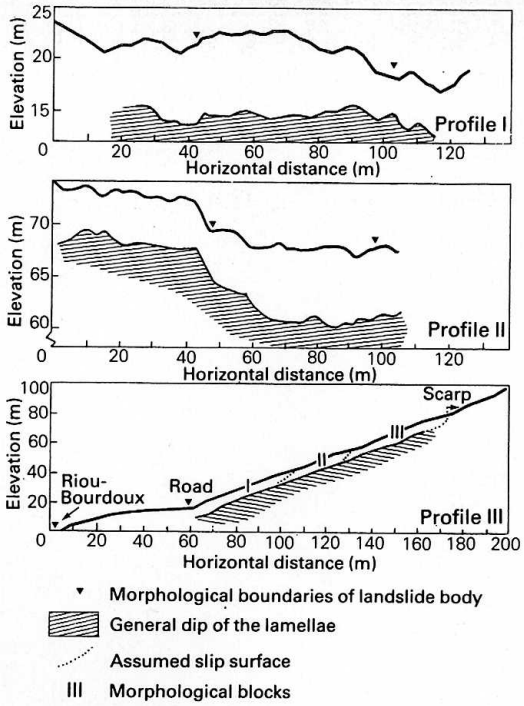

Fig.9. Depth to bedrock as calculated from the seismic refraction survey.

TABLE II

Comparison of electrical resitivities and velocities of longitudinal waves of bedrock and rock in the landslide body

Rock type	Electrical resistivity (Ohm·m)	V_p (m/s)
Rock in the landslide body	10–50	304–379
Bed rock	75–150	2586–3049

seismic profiles appear to be reliable. The surveys also indicate accumulation of water close to the bed rock, thus it may be assumed that the basal slip surface coincides with bed rock depth as determined at the refraction seismic profiles. These profiles can thus be used as an input for the stability analysis.

STABILITY ANALYSIS

Table I gives the geotechnical properties of the Terres Noires colluvial material. The peak strength values were obtained from nineteen drained triaxial tests, which

were run at 0.25 mm/hr deformation rate with consolidation pressures varying between 20 and 200 kPa. (Hazeu, 1988). The residual strength values of the colluvium were estimated by the assessment of an apparent threshold value for 24 creep tests (Van Asch et al., 1989). The stability calculations were carried out for different groundwater conditions using the simplified Janbu method. The probability of failure was determined according to the method given by Lee et al. (1983) assuming a normal distribution for the strength values (Mulder and Van Asch, 1985). It was assumed that the form of the slip surface follows the boundary between the weathered and unweathered material surveyed by refraction seismics. Results of the stability calculations are given in Fig.10 and Table III. Figure 10 shows that initial failure of the total landslide (under peak strength conditions) may have occurred when the groundwater was near the ground surface. In that case, the probability of failure appears to be 30%. Figure 10 also shows that the actual total slide could be remobilized if the groundwater level rose to a height of 4 m below the ground surface, assuming residual strength conditions.

The morphological mapping of the landslide revealed that three blocks can be distinguished in the landslide (Fig.3). Table III gives an overview of the results of the stability analysis of these blocks. The groundwater level was assumed to have a constant depth below the ground surface. It shows that there is no significant difference in stability between a section of the landslide and the total landslide complex. However, morphological observations showed that the lower block (Fig.3) appears to have moved independently from the rest of the landslide. This can be

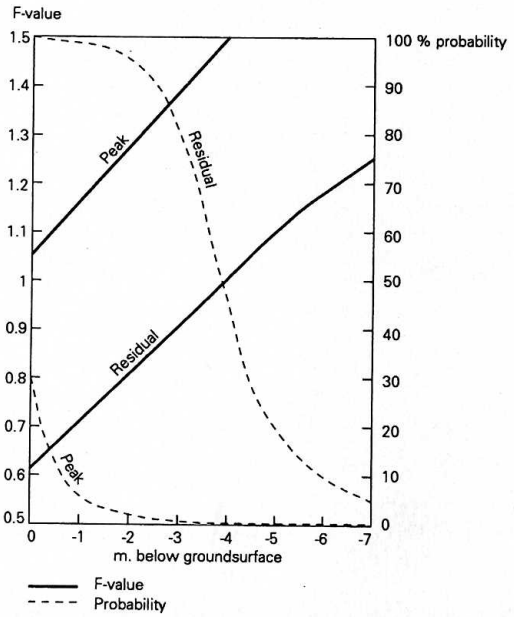

Fig.10. The relation between the depth of the groundwater level below the ground surface and the mean safety factor and probability of failure of the landslide.

TABLE III

The mean safety factors and the probability of failure for different conditions of the landslide. A = stability for peak strength conditions with the groundwater level at the surface, B = stability for residual strength conditions and the groundwater level at 4 m below the ground surface

	Block I		Block I+II		Block I+II+III	
	F value	Probablility (%)	F value	Probablility (%)	F value	Probability (%)
A						
Forest	1.09	20.9	1.09	19.7	1.05	30.6
After logging	1.07	26.3	1.07	25.5	1.03	37.3
No root strength	1.06	26.6	1.07	25.7	1.03	37.5
B						
Forest	1.03	38.8	1.04	36.9	1.00	46.9
After logging	1.02	42.5	1.03	40.5	1.00	50.3
No root strength	1.02	43.3	1.03	40.5	1.00	50.6

explained by a higher groundwater level during failure in the lower part in comparison with the upper part of the landslide.

The mechanical effect of the forest cover on the stability of the landslide complex is also indicated in Table III. The removal of an estimated forest load of 5 kN/m^2 has resulted in a slight decrease in stability (see "logging" in Table III). These calculations also show that the effect of a decrease in root strength on the stability can be neglected (see "no roots", Table III).

The removal of the forest cover may cause a rise in maximum pore water pressure due to a decrease in transpiration and interception losses, causing higher maximum groundwater levels. An assumed maximum rise in the groundwater of 0.5–1 m in the actual slide, due to deforestation, gives an increase in the probability of failure of 15–30%, as can be seen in Fig.10.

HYDROLOGICAL INVESTIGATION

In the previous section it was indicated that variations in pore water pressure play an important role in temporal variations of the safety factor. The stability analysis revealed that, for renewed unstability to take place, the groundwater level has to rise to a height of 4 m below the ground surface. In this section, the processes governing the water flow in the slope investigated and the meteorological conditions giving rise to pore pressures resulting in instability will be discussed.

Field observations

Soil pits within the landslide body revealed that, during wet periods, moisture concentrates in macropores (for a review of macropores see Beven and Germann, 1982) whereas the interior of the aggregates is drier. In this case the macropores are

formed mainly by shrinkage cracks going down to a depth of approximately 1.5 m and to a lesser extend by pores formed by the soil fauna and by plant roots.

At the landslide body several well defined locations were found where water is slowly seeping to the ground surface even after several days without rain. The water infiltrates again in the immediate vicinity of these small seepages. It has also been noted that, under wet conditions, some boreholes would fill almost completely with water within a day, whereas other boreholes remained dry. Once, during heavy rainfall, water draining out of a pipe which was located in the main head scarp of the landslide was observed.

These observations illustrate that macropores provide a means for rapid water transport in the upper 1.5 m of the landslide. According to Kirkby (1988), these non-capillary voids may behave as a dendritic network. This network carries a high proportion of the total hillslope flow towards a relatively small number of discrete seepage lines, which are difficult to recognise.

Since the amount of macropores rapidly decreases between a depth of 1 and 1.50 m, a rapid decrease in vertical permeability can be expected which favours the development and persistence of a perched water table (Weyman, 1973), inhibiting rapid percolation deeper into the landslide body.

Saturated hydraulic conductivity

To evaluate the decrease in permeability, the inversed auger hole method was used to measure saturated hydraulic conductivity (K_{sat}) at two different depth intervals during a relatively dry period when no water was observed to flow into boreholes.

The principle of the auger hole test above the water table consists of boring a hole to a given depth, filling it with water, and measuring the rate of fall of the water level (International Institute for Land Reclamation and Improvement, 1974). The results are summarized in Table IV. In four boreholes the water level fell so fast that it was impossible to measure the rate of fall of the water level. This illustrates the important influence of macropores on the saturated hydraulic conductivity. The Wilcoxon two-sample test, with a significance level of 0.001, was carried out to the measured values of K_{sat}. This test showed that the saturated hydraulic conductivity from 0.3 to 0.8 m depth is significantly higher than that from 1.5 to 2.0 m depth.

TABLE IV

Mean value and standard deviation of saturated conductivity for two depth intervals as determined with the inversed auger hole method

Depth (m)	n	K_{sat} (cm/day)	Sk_{sat} (cm/day)
0.3–0.8	11*	15.7	12.0
1.5–2.0	8	0.7	1.5

*In four other boreholes no measurement was possible due to the rapid fall of the water level in the upper half of the boreholes.

Below 2 m, a decreasing trend in permeability, due to increasing compaction of the soil material with depth, may be expected. To measure the whole range of saturated conductivity for the upper layer with macropores the cube method of Bouma and Dekker (1981) was used. An additional advantage of this method is that it measures horizontal and vertical K_{sat} separately, whereas the inversed auger hole method measures an undefined mixture of horizontal and vertical flow components.

The cube method: A cube of soil ($25 \times 25 \times 25$ cm) is carved out in situ and covered with gypsum. A vertical K_{sat} is measured by infiltrating water into the exposed upper surface and collecting it below the exposed lower surface of the cube (Fig.11). Measuring K_{sat} in two directions in the same sample as described by Bouma and Dekker posed too many problems. Therefore, to measure horizontal K_{sat} separate samples were carved out, turned on their side and covered with gypsum. In this case, the vertically measured K_{sat} represents the horizontal K_{sat} of the cube in its original position in the soil. The results in Table V illustrate the high permeability in a vertical and horizontal direction of the upper layer with macropores.

Much lower values of K_{sat} were measured with the inversed auger hold method.

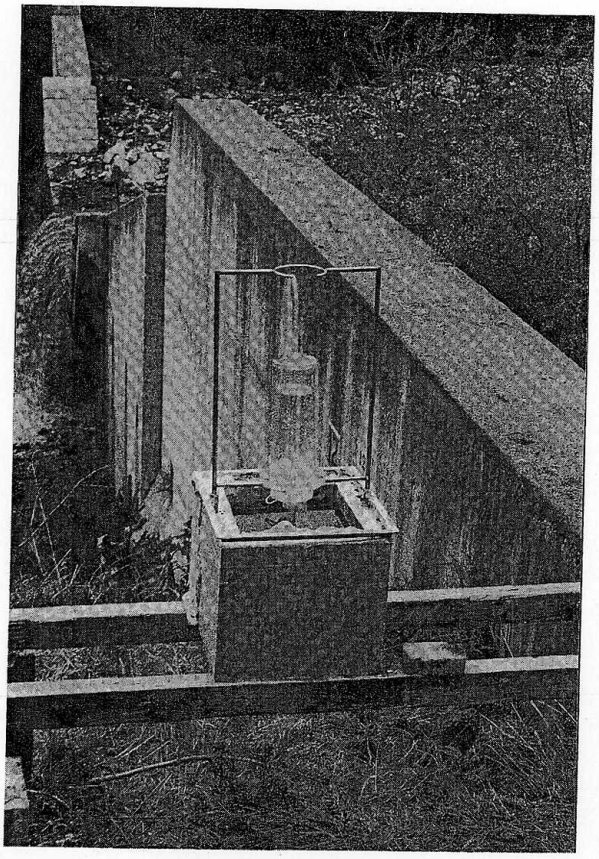

Fig.11. Gypsum-covered cube of soil, used to measure the vertical or horizontal K_{sat}.

TABLE V

Horizontal and vertical K_{sat} from 0.25 to 0.50 m as determined with the cube method in four different samples

Horizontal K_{sat} (cm/day)	Sample No.	Vertical K_{sat} (cm/day)	Sample No.
150	1	6376	3
397	2	23	4

Since the amount and dimensions of the macropores decrease with depth, the lower values resulting from the inversed auger hole method can partially be explained by the larger depth interval over which K_{sat} is measured (0.3–0.8 versus 0.25–0.5 m — with the cube method). This is especially true considering that the top 80 cm is not homogeneous, because the root zone (the layer with 80% of the roots) was found at a depth of 0.4–0.6 m (Mulder and Van Asch, 1988). Furthermore, extremely high flow velocities, as observed in four inversed auger hole measurements, could not be taken into account because no K_{sat} values could be determined from these tests. From this, it may be concluded that the cube method gives the correct values for K_{sat} in the root zone, whereas the inversed auger hole method yields correct values of K_{sat} for the layer without macropores, from 1.5–2 m. However, to give a correct value of the K_{sat} for the layer from 0.5 to 1.5 m extra measurements will be necessary.

The main conclusion is that a significant decrease in permeability occurs in the upper 1.5 m and that the permeability of this upper layer is mainly controlled by macropores.

Soil water pressure head

To measure soil water tension, 23 tensiometers were installed in three plots. Tensiometer nest 1 was installed at the crossing of profiles I and III (Fig.3). Tensiometer nest 2 was installed at the crossing of profiles II and III. Tensiometer nest 3 was installed north of tensiometer nest 1 in the stable part of the slope.

To install the tensiometers (maximum depth 6 m) an oversized hole ($\Phi = 5$ cm) was drilled to the required depth. The tensiometer was then lowered into the borehole after which the hole was filled up with dry loess to a depth of 5 cm above the cup. The loess was used to ensure:

(1) good hydraulic contact between the soil and the cup;

(2) sufficient unsaturated hydraulic conductivity during high water tension.

The hole was sealed by backfilling the lower part of the hole with bentonite grains after pouring water on the loess. The upper part of the hole was backfilled with the original soil material.

So far, only measurements taken in May 1989 are available. Since precipitation in this month was very low (compare Fig.2 and Fig.12) the tensiometer measurements were made at an interval of several days. The results of tensiometer nest 1 in Fig.13 show a wet upper layer up to a depth of 1.5 m which dries slowly. This upper layer is underlain by relatively dry soil which gradually becomes wet. Despite the large

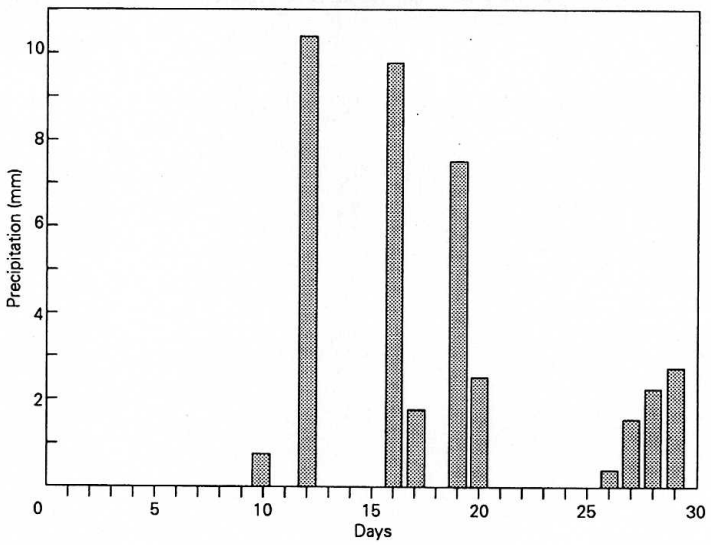

Fig.12. Precipitation at the study site for May, 1989. Precipitation was measured with an autographic rain gauge.

hydraulic gradient between the upper layer and the subsoil, there is only slow vertical drainage of water due to the very low unsaturated hydraulic conductivity of the dry subsoil. The results of the measurements taken at a depth of 6 m, are available for the second half of the month. These results indicate that, towards the bed rock, the soil becomes moister again, which was also indicated by the resistivity measurements. If the soil at 6 m is in equilibrium with the water table, then this water table must be at a depth of approximately 7.25–7.50 m. This is feasible, since at this location the seismic data indicate that depth to bed rock is 8.25 m.

Malfunctions of some tensiometers in tensiometer nests 2 and 3 produced incomplete data for the second half of the month, and for this reason only the measurements of the first half of the month will be discussed. The results of tensiometer nest 2 for the upper 1.5 m are comparable with tensiometer nest 1. However, at tensiometer nest 2, saturated zones lasting for several weeks were measured at 2.5 and 3 m with a maximum depth of 0.3 m above the tensiometer level. The deepest tensiometer, at 4.3 m, again indicated unsaturated conditions, which are also indicated by the resistivity log at this point (see Fig.7, borehole 3). Initially, bad sealing, allowing water to flow down the holes with tensiometers, was thought to be responsible for the measured saturated conditions. However, after carefully installing another tensiometer at 3 m, the same saturated conditions were observed. As yet no satisfactory explanation has been found for this phenomenon.

Tensiometer nest 3 on the stable part of the slope indicates a relatively moist layer, 1 m thick, whereas initial water tensions of around 6.5 m were measured at 1.5 and 2 m depth. A relatively moist layer underlain by a very dry layer coincides with the shallow resistivity soundings on this part of the slope (Fig.4A).

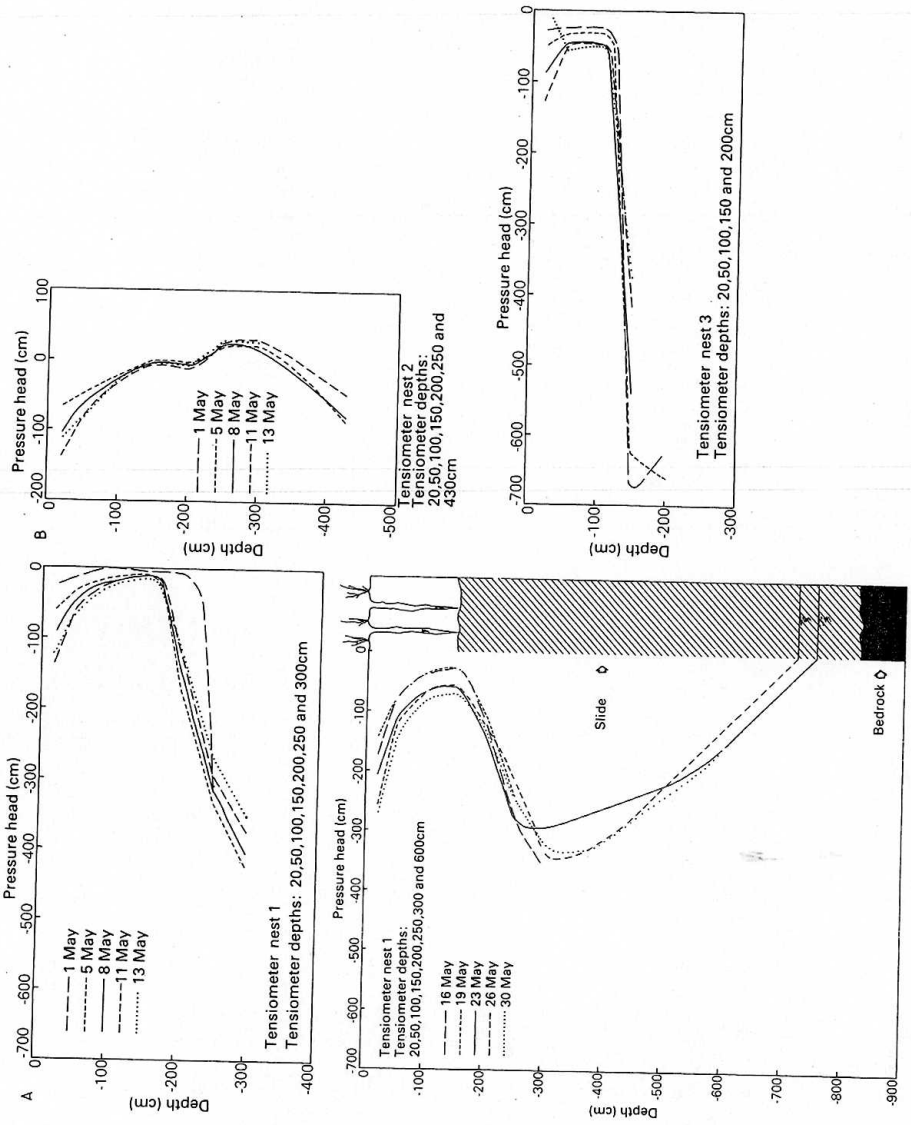

Fig.13. Pressure heads measured with tensiometers at three sites in May, 1989. For tensiometer nest 1 the soil profile is also shown.

DISCUSSION

The geophysical and hydrological investigations show that the major part of the landslide body is unsaturated. The moisture concentrates in the upper layer with desiccation cracks and in the zone close to the bed rock. The relatively dry, poorly permeable, intermediate layer (roughly from 1.5 to 4–9 m) is situated underneath the rooting zone and above the impervious bed rock. Therefore, the high water tensions found in this zone can only be explained by long-term, slow down-slope drainage of this layer. At the same time, the data show that relatively fast subsurface run-off of excess rainfall occurs within the highly permeable upper 1.5 m of the landslide body in which a perched water table may occur.

On the stable slope, conditions are drier and no saturated zones have been found. This is probably due to the higher tree density resulting in more interception and higher transpiration losses. It seems unlikely that there is a slow infiltration of water into the landslide body from other parts of the slope, due to the drier conditions of these stable slopes and the general dip of the lamellae (see Fig.9).

The stability analysis shows that a continuous phreatic surface at a depth of 4 m below the ground surface is necessary for the initiation of new movements of the whole landslide or parts of it, assuming that the slip surface is in a state of residual strength.

The above shows that this condition does not result from short-term heavy rainfall events, because most of the water will be rapidly transported down-slope through the upper layer. Only during long-term wet conditions with limited evapotranspiration can the slow vertical drainage be maintained, which can eventually cause unstability.

Thus, it is obvious, that the placing of interception drains in the permeable upper 1.5 m of the landslide is probably a sufficient preventive measure against the possible re-initiation of sliding, since without the infiltration from the upper layer, no critical pore water pressures can build up above the basal slip plane.

CONCLUSIONS

The combination of several geophysical methods (electromagnetic, geo-electric and refraction seismic) allowed location of the basal slip plane. The slip plane has been used as input for a detailed stability analysis. Furthermore, the data indicated differences in water content between the stable and unstable parts of the slope and within the landslide body. The advantages of these sorts of data are that they can be available almost instantaneously, at relatively low cost, and with little or no disturbance of the processes being investigated.

Stability analysis revealed that initial movement of the landslide must have occurred with the groundwater level at the ground surface. Renewed movements under residual strength conditions can take place if the groundwater level rises to a depth of 4 m below the ground surface. The effect of forest vegetation on this type of landslide is limited.

The saturated hydraulic conductivity measurements and field observations

underline the important role of macropores, whose influence on hydrological processes are still difficult to measure and model on a field scale. Furthermore, the measured permeabilities and pressure heads indicate that, in this material with low matrix conductivities, long-term meteorological conditions may play a more important role than the short-term heavy rainfall events which are generally used to explain unstability.

The placing of interception drains in the upper 1.5 m of the landslide body is probably a sufficient remedial measure against renewed sliding.

ACKNOWLEDGEMENTS

The authors are indebted to Dr. D.T. Bieuwinga, Drs. T. Stavenga, Ing. T. de Beer and Prof. Dr. K. Helbig for introducing the first author into geophysics and for their constructive remarks. We would also like to thank Ir. J.W. Bakker, Mr. W. Verhaegh, Dr. Ir. C. Dirksen and Dr. J.A. van den Berg for their support and valuable suggestions on hydrological matters and Mr. R. Hoogendoorn and Mr. J. Blokzijl for their advice regarding drilling techniques.

We are indebted to Mr. C.J.M. Klawer, Mr. W.J.C. Haak and Ing. Th.G.M. Tiemissen for the preparation and improvement of field equipment, and we are also grateful to the students: Miss M. Braam, Miss J.C. Pleumeekers, Mr. C. Stiggelbout, Mr. H. Kruse, Mr. M. Verschoor, Mr. D. Bravenboer and Mr. M.T.J. Terlien for their efforts during the field work, and Drs. Leonie van der Maesen and Mrs. Eugenie Kos for editing the English text.

Part of this research was funded by the Centre National de la Recherche Scientifique (CNRS) on the proposal of the Netherlands Organization for Scientific Research (NWO).

APPENDIX: FIELD ARRANGEMENT, ALGORITHM AND FIELD DATA OF THE REFRACTION SEISMIC SURVEY

Field arrangement

The distance between geophone stations is 2.5 m for the traverse profiles and 4 m for the longitudinal profile. An overlap of two geophones was used between succeeding spreads (Fig.14). Offset shots were used for most spreads to obtain first arrivals

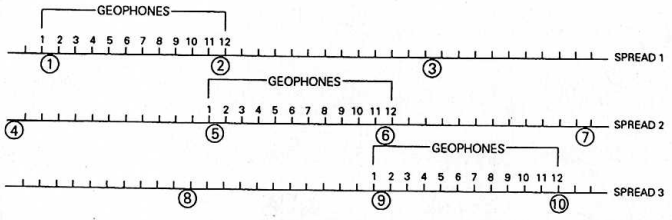

Fig.14. Field arrangement of a refraction profile. *1,2,5,6,9,10* = near-shot points; *3,4,7,8* = offset-shot points.

from the refractor at all geophone stations. To correct the irregular surface the elevation differences between the geophones were measured.

Algorithm

The algorithm will be demonstrated using synthetic data (Fig.15). To elaborate the data the forward branches of a profile are linked together on transparent paper by parallel shifting of the travel-time curves. The same is done for the reverse branches, but they are drafted from left to right, like the forward branches. The sheet with the linked reverse travel-time curves is superimposed on the forward travel-time curves and rotated. This produces a plot with inverted time axis and shifted origin (see Figs.15A–C). The minus-times are the midpoints between the two branches, and the plus-times are represented by the distance of (either) high-velocity branch from this line. When data are plotted in this format, the determination of plus- and minus-times consists of the determination of the median line. The average slope of this median line is a good approximation of the refractor velocity (Fig.15D). The conversion to "orthogonal distances" is done by dividing the product of plus-time and the velocity of the first layer by the cosinus of the critical angle. To find the base of the structure below the surface, circles should be drawn with the surface points as centers and the orthogonal distances as radii. Eventually the common envelope to these circles is drawn and identified with the refractor (Fig.15E).

Field data

The field data (Fig.16) show only two layers (i.e. one interface). Due to the high degree of seismic contrast (the mean velocity of the first layer is 340 m/s and the mean velocity of the refractor is 2780 m/s) the cosinus can be equalized with 1. The orthogonal distances are therefore equal to 340 multiplied with the plus-time at every point. The measured velocity of 340 m/s probably does not represent the velocity of the compressional seismic wave in air because: (1) 340 m/s is in the range of velocities typical for soft, unconsolidated surface deposits (i.e. 200–400 m/s) and (2) a much

Fig.15. Illustration of the graphical elaboration of the plus-minus method with synthetic data (From Helbig, 1987). A. Synthetic structure used to illustrate the graphical method. Velocity ratio is assumed to be 1:2 (critical angle $i_c = 30°$). B. Travel-time curves corresponding to two refraction observations from left to right and from right to left over the synthetic structure shown in A. C.Time–distance loop with intermediate observations based on B. All points of origin lie on the "opposite" travel-time curve. D. Plus-times (bars) (half the length of the vertical bars) and minus-times (dots) in a pair of travel-time curves plotted with inverted time axis. The figure has been obtained by supplementing C. The open circles on the travel-time curves are intermediate source points (with the corresponding x- and t-axes), the broken-line and the dash-double-dot line are the corresponding low velocity branches. E. The envelope to circles with the orthogonal distances determined from the plus-times of D matches the model structure (dots) closely.

lower or higher velocity does not coincide with the depths found with the borings and geo-electric soundings.

Towards the edges of the profiles only one high-velocity branch is available. In this case the median line can only be approximated (crosses in Fig.16C) by the

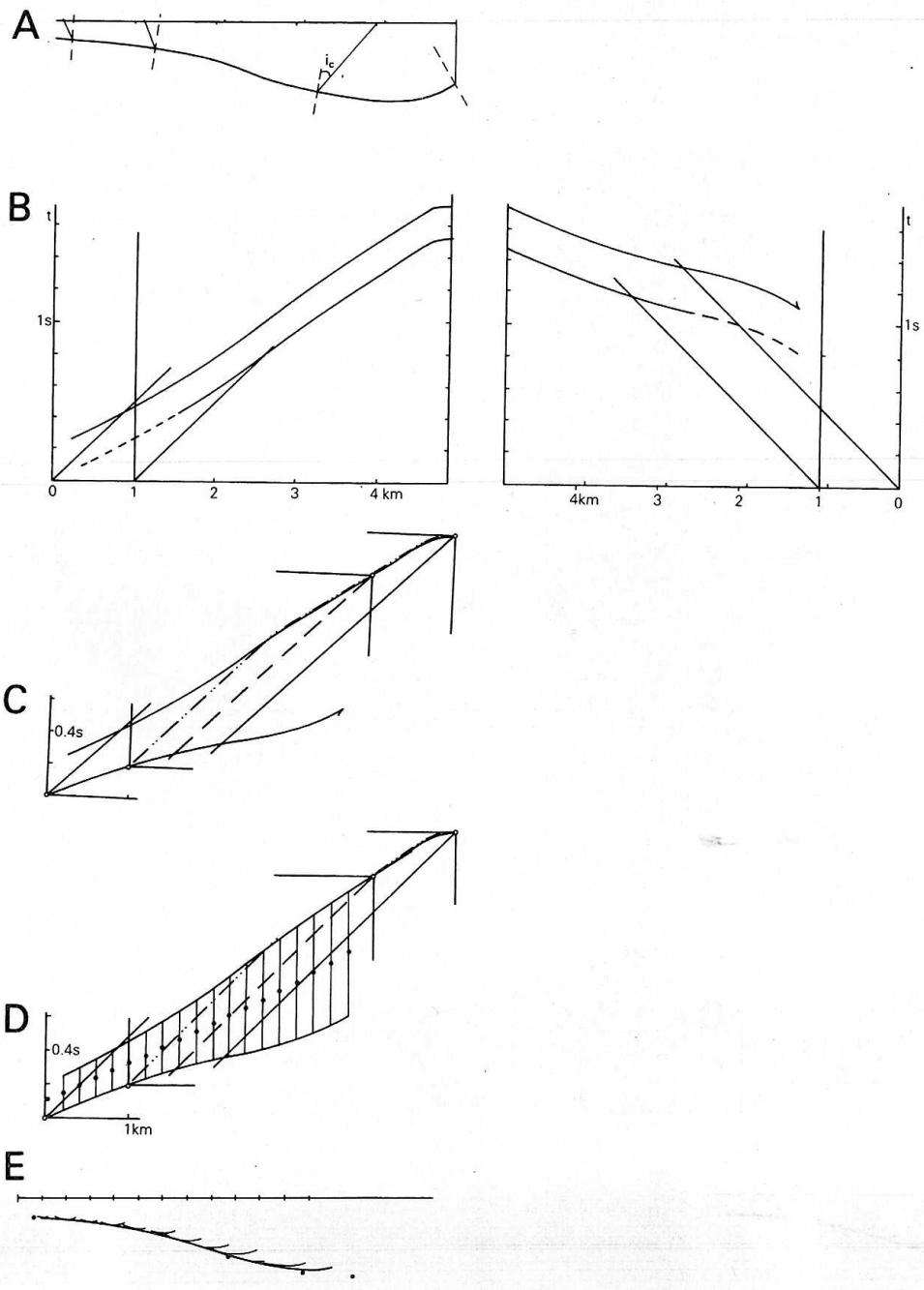

extension of the median line based on two high-velocity branches (circles in Fig.16C). Consequently, the orthogonal distances based on the extension of the median line are less accurate.

REFERENCES

Anon., 1976. Torrent du Rioux-Bourdoux. Serie domainale de Saint Pons (Basse Alps).

Beven, K. and Germann, P., 1982. Macropores and water flow in soils. Water Resour. Res., 18 (2): 1311–1325.

Bouma, J. and Dekker, L.W., 1981. A method for measuring the vertical and horizontal K_{sat} of clay soils with macropores. Soil Sci. Soc. Am. J., 45: 662–663.

Bogoslovsky, V.A. and Ogilvy, A.A., 1977. Geophysical methods for the investigation of landslides. Geophysics, 42 (3): 562–571.

Hagedoorn, J.G., 1959. The plus–minus method of interpreting seismic refraction lines. Geophys. Prospect., 7: 286–294.

Hazeu, G.W., 1988. Grondmechanische proeven op morene materiaal. Msc. Thesis, Dep. Physical Geography, Univ. Utrecht, Netherlands.

Helbig, K., 1987. Refraction seismic. Syllabus Dep. Exploration Geophysics, Univ. Utrecht, Netherlands, 162pp.

Hutchinson, J.N., 1982. Methods of locating slip surfaces in landslides. Technical Bull. Br. Geomorphol. Res. Group, 30, 30pp.

International Institute for Land Reclamation and Improvement, 1974. Drainage principles and applications. Vol. III. Surveys and Investigations. I.L.R.I, Wageningen, Netherlands, Publ. 16, pp.292–296.

Kirkby, M., 1988. Hillslope runoff processes and models. J. Hydrol., 100: 315–339.

Lee, I.K., White, W. and Ingles, O.G., 1983. Geotechnical Engineering. Pitman, Boston, Ma., 508pp.

McNeil, J.D., 1980. Electromagnetic terrain conductivity measurement at low induction numbers. Technical Note TN-6, Geonics, Mississauga, Canada, 15pp.

Mulder, H.F.H.M. and Van Asch, Th.W.J., 1988. On the nature and magnitude of variance of important geotechnical parameters, with special reference to a forest area in the French Alps. In: C. Bonnard (Editor), Landslides, Proc. Int. Symp. on Landslides, 5th (Lausanne, Switzerland), Balkema, Rotterdam, Vol. 1, pp.239–245.

Salomé, A.I. and Beukenkamp, P.C., 1988. Geomorphological mapping of a high-mountain area, in black and white. Z. Geomorphol., 33(1): 119–123.

Thornthwaithe, C.W. and Mather, J.R., 1957. Instructions and tables for computing potential evapotranspiration and the water balance. Climatology, 10 (3): 185–311.

Van Asch, Th.W.J., Deimel, M.S., Haak, W.J.C. and Simon, J., 1989. The viscous creep component in shallow clayey soil and the influence of tree load on creep rates. Earth Surf. Processes Landforms, 14: 557–564.

Weyman, D.R., 1973. Measurement of downslope flow of water in a soil. J. Hydrol. 20: 267–280.

pp.273–276

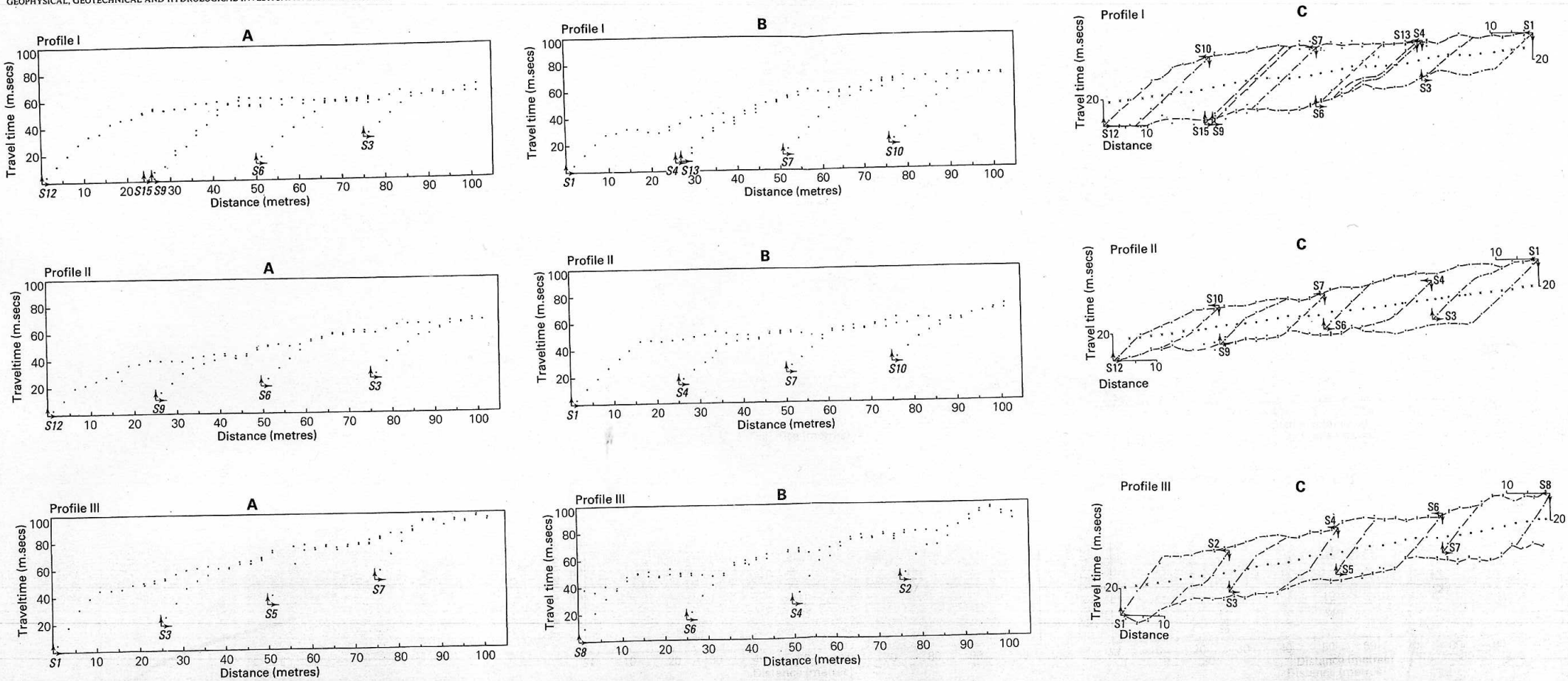

Fig.16. Graphical elaboration of three refraction seismic profiles. A. Linked forward branches. B. Linked reverse branches. C. Travel-time curves plotted with inverted time axis. Circles in the median line indicate minus times; crosses indicate minus times based on extension of the median line.